Int. J. Microgravity Sci. Appl., **35** (4) (2018) 350402
DOI: 10.15011//jasma.35.350402

IIII Original Paper IIII

Investigation of the Influence of Different Solute on Impurity Diffusion in Liquid Sn using the Shear Cell Technique

Noriyuki YAMADA[1], Shinsuke SUZUKI[2], Koji SUZUKI[1],
Anna TANAKA[1], Rie MORITA[1], Chenglin CHE[1] and Günter FROHBERG[3]

Abstract

Impurity diffusion coefficients D of five kinds of solute elements in liquid Sn were measured using the Foton shear cell with stable density layering on the ground. This experiment involved diffusion from a thin alloy layer of 3-mm thickness into pure Sn. The Sn alloys contained Ag, Bi, In, Pb, or Sb at 5at%. The diffusion couple was set vertically so that the side with higher density was on the bottom, which is called stable density layering. Four identical parallel experiments were performed simultaneously for each condition. The diffusion temperature was 573 K, and the diffusion time was 8 h. Each obtained profile agreed well with the theoretical equation for the thick layer solution of the diffusion equation (coefficient of determination $r^2 > 0.999$). The reproducibility of the diffusion coefficients among the four parallel experiments was very good with a standard deviation less than 2.5%. The obtained diffusion coefficients D_{Bi} and D_{In} agreed well with μg-reference data. Therefore, the buoyancy convection was assumed to be suppressed by the stable density layering during the diffusion experiments in this study, including the experiments of SnPb, SnAg, and SnSb with high density gradient. The impurity diffusion coefficients in liquid Sn at 573 K can be expressed as a proportional relationship to the product of the ratio of atomic radii r_s/r_i of the two substances and thermodynamic factor ϕ_{is}, with a gradient equivalent to the value of the self-diffusion coefficient of Sn.

Keyword(s): Shear cell, Impurity diffusion, Sn, Ag, Bi, In, Pb, Sb, Microgravity, Liquid metal

Received 18 September 2018, accepted 24 October 2018, published 31 October 2018.

1. Introduction

The diffusion coefficients of liquid metals are very important in the study of crystal growth and solidification. However, the diffusion mechanism in liquid metals is not yet fully understood. In the theoretical research of diffusion in liquid metals, models assuming a lattice point in liquid have been proposed since 1940s[1,2]. However, presently, no theory quantitatively predicts the diffusion coefficients. Some researchers have concluded that diffusion coefficients will become large if the atomic radius of the impure component is smaller than that of the solvent[3-5]. However, the accuracy of the experimental data used in those studies is not sufficient to discuss the diffusion mechanism because the concentration profiles used were disturbed and the error ranges were large. In addition, these theories do not consider the effect of the interaction between the impure solute component and solvent atoms. According to the theory regarding the gradient of the chemical potential, the diffusion coefficient is a function of the thermodynamic factor ϕ. The validity of this theory was already confirmed in crystal metals [6].

The experimental measurement of diffusivity in liquid metals is difficult because convection deteriorates the accuracy of the experimental results. This is one of the main reasons for the limitation of available and reliable experimental data. To remove the disturbance of buoyancy convection from experiments, diffusion coefficients have been measured using the shear cell technique in microgravity, for example, Spacelab-D1(SL-D1) [7], TR-IA [8-9], MSL-1 [10-11], Foton-12 [12], and Foton-M2 [13-17]. Details of the advances in diffusion experiments in microgravity are described in a review paper [18].

On the other hand, the technique for the suppression of convection was developed for ground experiments. The experimental method using the shear cell technique with stable density layering enabled us to suppress buoyancy convection and Marangoni convection, and thus, measure the diffusion coefficients accurately on the ground [19-22]. This experimental method helps to accumulate the basic diffusion data, which are used for investigating the theory of diffusion.

This study was aimed at investigating the effect of impure solute on the diffusion in liquid metals. We measured the impurity diffusion coefficients of Ag, Bi, In, Pb, and Sb in liquid Sn using the shear cell technique with stable density layering. Then, we compared the obtained diffusion coefficients with a theoretical formula containing the thermodynamic factor ϕ.

1 Faculty of Science and Engineering, Waseda University, Tokyo 169-8555, Japan.
2 Department of Applied Mechanics and Aerospace Engineering and Kagami Memorial Research Institute of Materials Science and Technology, Waseda University, Tokyo 169-8555, Japan.
3 Professor Emeritus, Technishce Universität Berlin, 10623 Berlin, Germany.
(E-mail: suzuki-s@ waseda.jp)

2. Experimental Procedure

Figure 1 shows the shear cell used in this study, which is the same type as that used in the Foton-M2 [13-17] and applicable to experiments on the ground [19-22]. The shear cell unit had an outer cylinder, an inner cylinder, and 20 graphite disks of 3-mm thickness; each with four capillaries of 1.5-mm diameter. The two types of disks (**Fig. 2**), were connected alternately. By connecting these disks, a capillary with length of 60 mm was formed. On both ends of the capillary, reservoirs were equipped.

The experimental procedure using the shear cell technique is shown in **Fig. 3** [19-22]. The type of experiment was diffusion from a thin alloy (Sn-Ag, Sn-Bi, Sn-In, Sn-Pb, and Sn-Sb) layer of 3-mm thickness into pure Sn. As **Fig. 4** shows, the higher density sample was set on the bottom, that is, Sn-Ag, Sn-Bi, and Sn-Pb alloys were placed on the bottom, while Sn-Sb and Sn-In were set on the upper side. The samples were vertically arranged as a one-dimensional diffusion couple with the diffusion axis on its centerline. Two kinds of solid samples were set in the shear cell by setting an intermediate cell apart from the diffusion axis at room temperature. The samples with the same composition as that in the capillary were set in both reservoirs with elastically compressed graphite felts. Then, the shear cell was set in a furnace, which was fixed so that the diffusion axis was vertical. After evacuation of the furnace, the shear cell was heated to 573 K, and the samples were homogenized for 1 h. Then, to start the diffusion phase, a motor was rotated and the intermediate cell was inserted. After maintaining the temperature at 573 K for 28,800 s, the capillary was separated into 20 cells and cooled. Four identical parallel experiments were performed simultaneously under each condition, using four capillaries in a shear cell unit.

After the end of the diffusion experiments, each sample piece was dissolved in aqua regia and analyzed with inductively coupled plasma-optical emission spectrometry (ICP-OES, Agilent 5100). Concentration profiles were obtained by plotting the analyzed concentration of each sample in the middle position of each cell.

Fig. 1 Photograph of the shear cell same as used in the Foton mission.

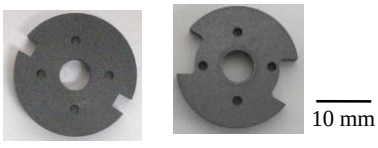

Fig. 2 Disks of the shear cell for uneven numbers (a) and for even numbers (b).

3. Results

Figure 5 shows the Ag concentration profiles obtained in these experiments. The mean square displacement $<X^2_{meas}>$ was calculated by fitting the theoretical formula of diffusion with error functions (Eq. (1)) to the obtained profiles. The diffusion coefficients D were compensated to eliminate the effect of averaging and shear convection following Eq. (2) [15,23].

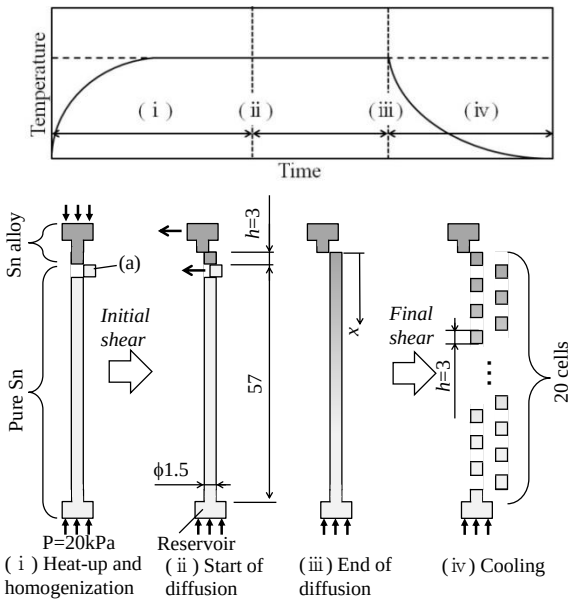

Fig. 3 Schematic illustration of the experimental procedure using the shear cell technique in this study. (unit: mm)

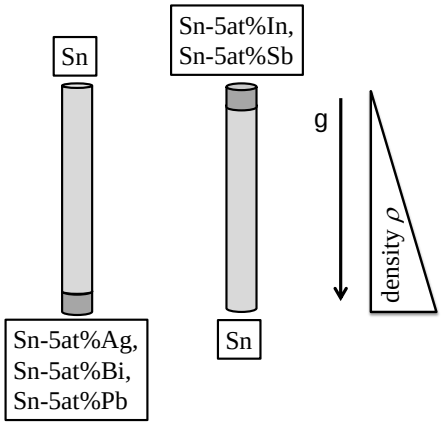

Fig. 4 Schematic illustration of setting the diffusion couple with stable density layering. The symbol g shows the gravity vector.

$$c(x,t) = \frac{c_0}{2}\left(\mathrm{erf}\left(\frac{h+x}{\sqrt{2 < X_{meas}^2 >}} \right) + \mathrm{erf}\left(\frac{h-x}{\sqrt{2 < X_{meas}^2 >}} \right) \right) \quad (1)$$

$$D = (< X_{meas}^2 > -2 \times 10^{-7} - 7.5 \times 10^{-7})/2t \quad (2)$$

Here, $c(x, t)$ is the concentration of the impurity at the position from the end (**Fig. 3(iii)**) at diffusion time t. The symbols c_0 and h are the initial concentration and thickness (**Fig. 3(ii)**) of the sample including the impurity, respectively.

Each obtained profile agrees well with the fitting function, with coefficients of determination r^2 larger than 0.999. The coefficient of determination r^2 is a parameter, which is calculated by subtracting 1 from the value and, thus, increases with increasing residual error of fitting. Therefore, a value of r^2 close to 1 means a good fit.

In addition, the reproducibility of the diffusion coefficients among the four parallel experiments was very good. There were small differences in the concentration at $x = 0$ mm. Small differences in both the initial condition c_0 and initial thickness h may have been the reason. However, when the concentration is normalized through division by the concentration at $x = 0$ mm, the curves overlap each other. Therefore, the difference in the concentration is negligible for the estimation of the diffusion coefficients.

The standard deviation of the diffusion coefficient was smaller than 2.5%. Garandet *et al.* [12] reported that the error of the impurity diffusion experiments in the Foton-12 mission, using a shear cell similar to the one used in this study, was 6% [12]. This value included a temperature measurement error of 2%, a convection error due to the g-jitter of 1%, and a concentration measurement error of 3%. The errors in measuring the temperature and time were not involved in this study because the experiments of the four couples were performed simultaneously. In addition, there was no influence of the g-jitter since the gravity direction is constant on the ground. The error factor in these measurements was only the measurement of the concentration, and the error value was similar to reference result reported by Garandet. Considering that the measurement error with ICP-OES was about 2%, we concluded that the obtained diffusion coefficients were highly reproducible.

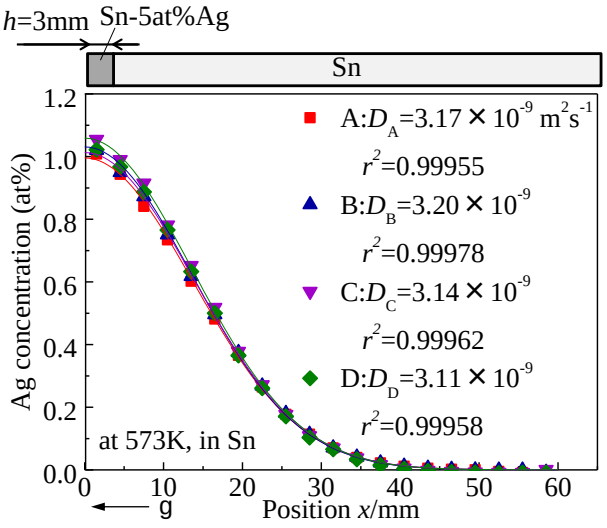

Fig. 5 Obtained concentration profiles of the four parallel experiments with Sn-5at%Ag. The position x is the distance from the end of alloy side. Solid lines are fitting curves. (g: gravity vector, r^2: coefficient of determination, suffix to the D: name of capillary, unit of D : $m^2 \cdot s^{-1}$)

4. Discussion

4.1 Suppression of convection

Frohberg reported that the diffusion coefficient is proportional to n-th power of the temperature with n ~ 2 [7]. The logarithm of the obtained diffusion coefficients was plotted against the logarithm of temperature in **Fig. 6** with the related reference data

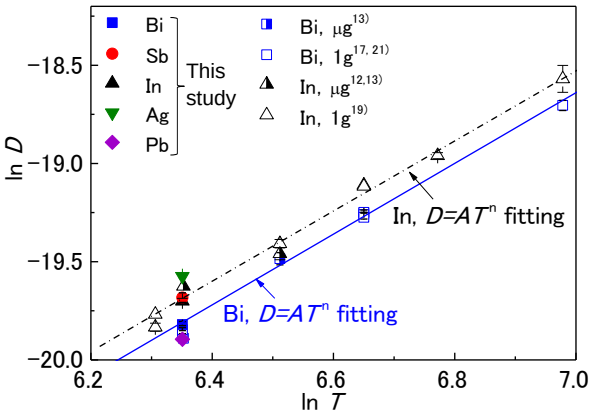

Fig. 6 Temperature dependence of the diffusion coefficients D in Sn: fitted lines obey $D=AT^n$.

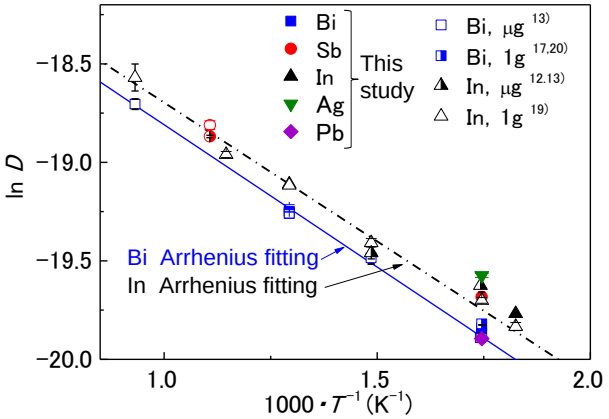

Fig. 7 Arrhenius plots of the diffusion coefficients D in Sn: fitted lines obey Arrhenius's law. (Unit of D : $m^2 \cdot s^{-1}$)

obtained from previous shear cell experiments on the ground [17, 19, 20] and in microgravity [12, 13]. The reference data were fitted by the power of the temperature dependence as Eq. (3).

$$D = AT^{n}. \tag{3}$$

Here, the symbols A ($m^2 \cdot s^{-1} \cdot K^{-n}$) and n are constants that vary according to the substance. The parameters (A, n) obtained by fitting the reference data were (2.61×10^{-14}, 1.80) and (3.40×10^{-14}, 1.78) for Bi and In, respectively. The lines in **Fig. 6** show the results of fitting the reference data. The obtained impurity diffusion coefficients of Bi and In in this study agree well with each of the lines.

In addition, **Figure 7** shows Arrhenius plots from Eq. (4) of the obtained data and reference data.

$$D = D_0 \exp(-Q/RT) \tag{4}$$

Here, the symbols D_0 ($m^2 \cdot s^{-1}$), Q ($kJ \cdot mol^{-1}$), and R ($kJ \cdot mol^{-1} \cdot K^{-1}$), are the pre-exponential factor, activation energy, and the gas constant, respectively. The parameters (D_0, Q) obtained by fitting the reference data were (2.934×10^{-8}, 12.16) and (3.109×10^{-8}, 11.72) for Bi and In, respectively. The obtained data of Bi and In also agree well with each of the Arrhenius plots.

Although these results are not the necessary and sufficient conditions for suppression of convection, if convection exists, the diffusion coefficients should be much higher than the fitting curves. Therefore, we considered that buoyancy convection was practically absent in these measurements.

However, there is no reference data for Ag and Pb using shear cell in microgravity, and the data for Sb have not been published. Therefore, we investigated the accuracy of these data considering the density distribution of these couples.

To discuss the dependency of density on concentration, data obtained from precise measurements are necessary. However, density data are not available currently. Thus, we considered that the following approximation of the density of a binary alloy can be applied to this study. For this calculation, a linear relationship between the density and concentration of the solute was assumed for the following reasons. First, the concentration region is narrow. Second, a magnitude relationship, rather than an exact numerical value, is needed in this study.

The density distributions of the samples were plotted against the longitudinal direction after the end of the diffusion experiments in **Fig. 8**. The density distributions were approximately calculated from the linearization of the density profile of Sn alloy with impurity between 0 at% (pure Sn) and 20 at% at 573 K [24-28]. The obtained equation is shown below.

$$\rho_{Sn-i} = \alpha_i \cdot N_i + \rho_{Sn} \tag{5}$$

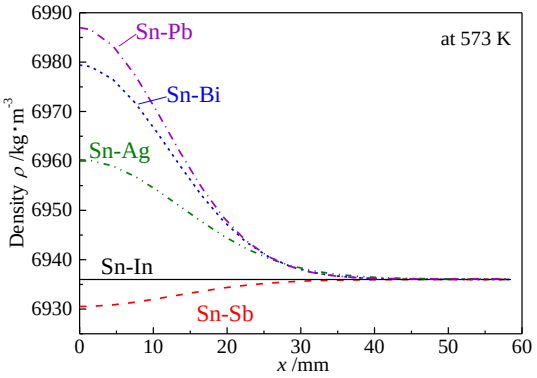

Fig. 8 Estimated density distributions of the samples after the end of the diffusion experiments. A linear relationship between density and concentration was assumed for the calculation.

Here, ρ is density and N_i is mole fraction of impurity. The suffix i represents the impurity element. The constant α_i is 2425 for Ag, 4876 for Pb, 4727 for Bi, -553.9 for Sb, and -1.50 $kg \cdot m^{-3}$ $at\%^{-1}$ for In. The density of pure Sn, ρ_{Sn}, is 6936.1 $kg \cdot m^{-3}$. The densities of Sn-Pb, Sn-Bi, and Sn-Ag alloys are higher than those of Sn. Therefore, these samples were situated at the bottom of the vertically arranged one-dimensional diffusion couple. Conversely, Sn-In and Sn-Sb alloys were situated on the bottom, because the density of Sn is higher than this sample.

The difference in the density between Sn-In alloy and Sn is the smallest in the couples used in this study. From the agreement of μg data and obtained data of In, it is considered that the buoyancy convection was suppressed in the experiment of this diffusion couple. Therefore, we assume that in the experiment of the diffusion couple where the difference in the density between the alloy and pure metal is larger than that of Sn-In and Sn, the buoyancy convection is suppressed. The impurity diffusion of Pb, Ag, and Sb in Sn was assumed to be measured accurately through suppressing the buoyancy convection because the difference in the density between each alloy and Sn is larger than that between Sn-In and Sn.

4.2 Effect of the solute on the diffusion coefficient

According to the theoretical thermodynamic formula, the impurity diffusion coefficients D_{is} of impurity i in solvent s can be expressed by Eq. (6) [29].

$$D_{is} = M_{is} k_B T \phi_{is} \tag{6}$$

Here, M_{is} is the mobility of impurity atom i in solvent s, k_B is Boltzmann constant, T is temperature, and ϕ_{is} is thermodynamic factor of impurity for atom i in solvent s. The thermodynamic factor ϕ_{is} is defined as following Eq. (7).

$$\phi_{is} = \left(1 + \frac{\partial \ln \gamma_i}{\partial \ln N_i}\right) \tag{7}$$

Here, γ_i and N_i are the activity coefficients of impurity atom i and the molar fraction of atom i in the solution, respectively. It is generally known that the self-diffusion coefficients (impurity i is identical to solvent s, in this case) are expressed by the Southerland-Einstein equation[30] as equations (8) and (9).

$$D_s = M_s k_B T \tag{8}$$

$$M_s = \frac{1}{4\pi r_s \mu_s} \cdot \tag{9}$$

Here, r_s and μ_s are the atomic radius and viscosity coefficient of solvent s, respectively. Therefore, assuming the viscosities μ of all the alloys used in this study are equal to μ_s at 573 K, since the alloys are dilute, mobility M_{is} for impurity i in solvent s can be assumed to be proportional to the ratio of the atomic radii between the solute and solvent. We thus proposed Eq. (10) as follows,

$$D_{is} = M_{is}\phi_{is} RT = m\frac{r_s}{r_i}\phi_{is} k_B T \cdot \tag{10}$$

Here m is a constant, which is related to the mobility.

As the first step, the diffusion coefficients were compared with the ratio of the atomic radii. The thermodynamic factor for the dilute solution is close to 1.0. Therefore, if it is assumed that the thermodynamic factor ϕ_{is} is equal to 1.0, the diffusion coefficient is considered to be proportional to the ratio of the atomic radii. The impurity diffusion coefficients were plotted against the ratio of the atomic radii of the solute and the solvent in **Fig. 9**. The atomic radii were approximated to be same as the Gold-Schmidt radius [31]. The error bar contains the standard deviation for four capillaries and the temperature measurement error. This shows the tendency that the diffusion coefficient increases with decreasing atomic radius of the impurity. However, this does not indicate a close relationship between the diffusion coefficients and the atomic radius. Therefore, it is thought that the thermodynamic factor would affect the impurity diffusion coefficients.

From these results, both the ratio of the atomic radii and thermodynamic factor ϕ_{is} were considered. Setting $r_s\ \phi_{is}/r_i$ as the abscissa axis, the diffusion coefficient was assumed to be proportional to the abscissa axis. The diffusion coefficients were plotted against the product of the ratio of the atomic radii r_s/r_i and thermodynamic factor ϕ_{is} in **Fig. 10**. The values of the thermodynamic factors were obtained from the activity coefficients calculated with Thermo-Calc™ and were assumed to be the average value between 0 at% and 5 at%.

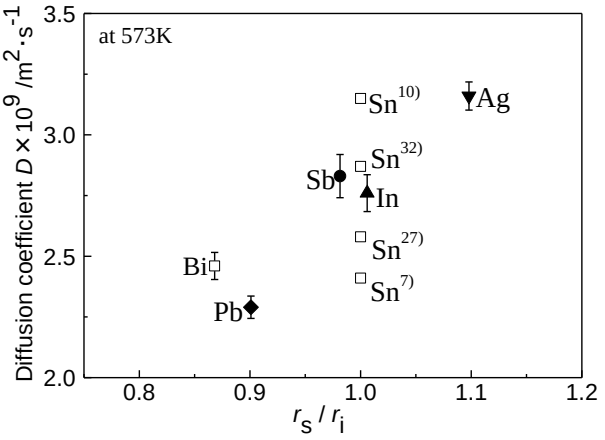

Fig. 9 Diffusion coefficients against the ratio of atomic radii, r_s(solvent)/r_i(impurity). The values of D_{Sn} were calculated by using the power law from the results of space shuttle missions[7,9] and shear cell experiments on the ground.

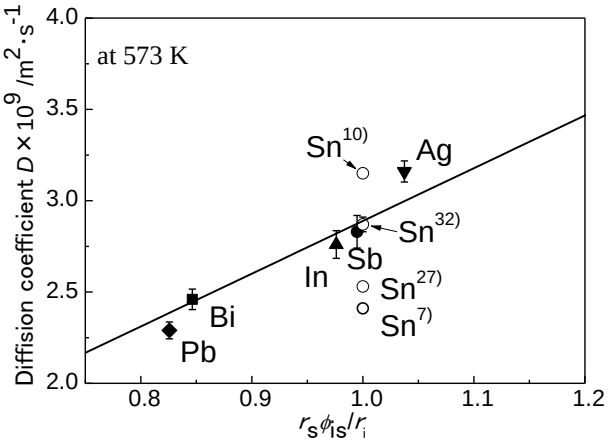

Fig. 10 Diffusion coefficients against the product of the ratio the of atomic radii r_s/r_i and thermodynamic factor ϕ_{is}. The solid line is the fitting line passing through the origin.

Table 1 Self-diffusion coefficients obtained by the n-th power law

D $\times 10^9$ m^2·s^{-1}	A $\times 10^{15}$ m^2·s^{-1}·K^{-n}	n	Temp. Range K	Apparatus (mission)	Ref.
2.41	7.33	2	543–1048	LC (SL-D1)	7)
3.15	32.5	1.81	900–1622	LC (MSL-1)	10)
2.52	6.91	2.02	543–1622	LC (SL-D1, MSL-1), SC (MSL-1)	10)

LC: long capillary, SC: shear cell, Temp. range: temperature range of measurements for fitting to the n-th power law $D = AT^n$.

4.3 Comparison with self-diffusion coefficient

Four values of the self-diffusion coefficient of Sn were plotted in **Figs. 9** and **10**. Three of them were calculated values by using the empirical formulas of the n-th power law (Eq. (5)) by fitting the experimental data in previous space shuttle missions, that is, the long capillary (LC) in Spacelab-D1 (SL-D1) [7], long capillary in MSL-1 [10], and shear cell (SC) in MSL-1 [11]. **Table 1** shows the values of D, the fitting parameters A and n, the temperature range of the measurements for the fitting, the names of the space mission, and the apparatus. The value $D_{Sn} = 2.41 \times 10^{-9}$ $m^2 \cdot s^{-1}$ was calculated by using the data of the SL-D1 mission [7]. The temperature range of the measurements was 543–1048 K. The value $D_{Sn} = 2.41 \times 10^{-9}$ $m^2 \cdot s^{-1}$ was calculated by using the long capillary data of the MSL-1 mission [10]. The range of temperature measurement was 900–1622 K, which was higher than that in the SL-D1 mission. The value $D_{Sn} = 2.52 \times 10^{-9}$ $m^2 \cdot s^{-1}$ was calculated by using the data of from the three experiments [10].

The relative error among the values of Sn self-diffusion was about 20%. This seems to be a good agreement. This may be due to differences in the experimental apparatus and measurement temperature range. The impurity diffusion coefficients are located in between the calculated self-diffusion data.

The fourth plot $D = 2.87 \times 10^{-9}$ $m^2 \cdot s^{-1}$ was obtained by using the same method as in our study [32]. For this comparison, the effects of the difference in apparatus and temperature were avoided.

A proportional function can be fitted well with the experimental data of impurity diffusion, with a high coefficient of determination $r^2 = 0.998$ and a gradient equal to 2.90×10^{-9} $m^2 \cdot s^{-1}$. Interestingly, this line was on the Sn self-diffusion coefficient profile obtained by the same method as in this study. Thus, the gradient of the line was in good agreement with the Sn self-diffusion coefficient.

Therefore, the impurity diffusion coefficients can be approximated as proportional to the product of the ratio of the atomic radii r_s/r_i and thermodynamic factor ϕ_{is}, with a gradient equivalent to the value of the self-diffusion coefficient of the solvent. From these results, it can be concluded that Eq. (10) can be applied to express the impurity diffusion coefficients. In this study, although r_s/r_i was varied, the range was narrow. Therefore, r_s/r_i can be approximated as 1 in Eq. (10). Under this approximation, the parameter m is the product of Avogadro's number and the mobility, which is in inverse proportion to the viscosity of the solvent.

In this study, only the impurity atoms in Sn, which have $r_s \phi_{is}/r_i \sim 1$, were used. The application of Eq. (10) for a combination of impurity and solvent with $r_s \phi_{is}/r_i$ far from 1 is the subject of a future study.

5. Conclusion

The impurity diffusion coefficients of Ag, Bi, In, Pb, and Sb in liquid Sn were measured at 573 K using the shear cell technique. From the four parallel experiments, high reproducibility (standard deviation < 2.5%) was demonstrated. The obtained data agreed well with the reference data measured using the shear cell. Therefore, this experimental procedure suppressed the buoyancy convection and measured the impurity diffusion coefficients accurately. The impurity diffusion coefficients in liquid Sn at 573 K can be expressed as proportional to the product of the ratio of the atomic radii r_s/r_i of the two substances and thermodynamic factor ϕ_{is}, with a gradient equivalent to the value of the Sn self-diffusion coefficient.

Acknowledgments

This study was supported by JSPS KAKENHI Grant Number 23560790, grant-in-aid from Iketani Science and Technology Foundation, Programs of Special Coordination Funds for Promoting Science, Japan Aerospace Exploration Agency Working group on "Diffusion Phenomena in Melts".

References

1) S. Glasstone, K.J. Laidler and H. Eyring: The Theory of Rate Processes, McGraw-Hill, New York, (1941).
2) R.A. Swalin, Acta Metall., **7** (1959) 736.
3) T. Ejima, N. Inagaki and M. Kameda: Trans. JIM., **9** (1968) 172.
4) A.K. Roy and R.P. Chhabra: Metall. Trans. A, **19A** (1988) 273.
5) J. Cahoon, Y. Jiao, K. Tandon and M. Chaturvedi: J. Phase Equil. Diff., **27** (2006), 325.
6) Th. Hehenkamp, W. Schmidt and V. Schlett: Acta Metall., **12** (1980) 1731.
7) G. Frohberg: Fluid Sciences and Materials Science in Space, Springer-Verlag, Berlin, 1987.
8) T. Itami, A. Mizuno, H. Aoki, Y. Arai, K. Goto, S. Amano, N. Tateiwa, M. Kaneko, T. Fukazawa, R. Nakamura, H. Nishioji, A. Ogiso, T. Nakamura, Y. Nakamura, N. Koshikawa, T. Masaki, M. Natsuisaka, S. Matsumoto, S. Munejiri, M. Uchida and S. Yoda: J. Jpn. Soc. Microgravity Appl., **17** (2000), 64.
9) K. Kinoshita, H. Kato, S. Matsumoto, S. Yoda, J. Yu, M. Natuisaka, T. Masaki, N. Koshikawa, Y. Nakamura, T. Nakamura, A. Ogiso, S. Amano, K. Goto, Y. Arai, T. Fukazawa, M. Kaneko and T. Itami: J. Jpn. Soc. Microgravity Appl., **17** (2000) 57.
10) T. Itami, H. Aoki, M. Kaneko, M. Uchida, A. Shisa, S. Amano, O. Odawara, T. Masaki, H. Oda, T. Ooida and S. Yoda: J. Jpn. Soc. Microgravity Appl., **15** (1998) 225.
11) S. Yoda, H. Oda, T. Oida, T. Masaki, M. Kaneko and K. Higashino: J. Jpn. Soc. Microgravity Appl., **16** (1999) 111. (in Japanese)
12) J.P. Garandet, G. Mathiak, V. Botton, P. Lehmann and A. Griesche: Int. J. Thermophys., **25** (2004) 249.
13) R. Roşu-Pflumm, W. Wendl, G. Müller-Vogt, S. Suzuki, K.-H. Kraatz and G. Frohberg : Int. J. Heat Mass Transfer., **52** (2009) 6042.
14) S. Suzuki, K.-H. Kraatz and G. Frohberg: Microgravity Sci. Technol., **18** (2006) 155.

15) S. Suzuki, K.-H. Kraatz and G. Frohberg: Microgravity Sci. Technol., **18** (2006) 82.
16) S. Suzuki, K.-H. Kraatz and G. Frohberg: J. Jpn. Soc. Microgravity, **28** (2011) S100.
17) S. Suzuki, K.-H. Kraatz, G. Frohberg, R. Roşu-Pflumm and G. Müller-Vogt, J. Non-cryst. Solids, **353** (2007) 3300.
18) T. Itami: J. Jpn. Soc. Microgravity Appl., **19** (2002) 185. (in Japanese)
19) S. Suzuki, K.-H. Kraatz and G. Frohberg: Ann. N.Y. Acad. Sci., **1027** (2004) 169.
20) S. Suzuki, K.-H. Kraatz and G. Frohberg: Microgravity Sci. Technol., **16** (2005) 120.
21) S. Suzuki, K.-H. Kraatz and G. Frohberg: J. Jpn. Soc. Microgravity Appl., **22** (1998) 165.
22) S. Suzuki, K.-H. Kraatz, G. Frohberg, R. Roşu-Pflumm, W. Wendl and G. Müller-Vogt: Ann. N.Y. Acad. Sci., **1077** (2006) 380.
23) S. Suzuki, K.-H. Kraatz and G. Frohberg: Microgravity Sci. Technol., **18** (2005) 127.
24) T. Gancarz, Z. Moser, W. Gąsior, J. Pstruś and H. Henein: Int. J. Thermophys., **32** (2011) 1210.
25) P.E. Berthou and R. Tougas: Metal. Trans., **1** (1970) 2978.
26) Z. Moser, W. Gąsior and J. Pstruś: J. Electron. Mater., **30** (2001) 1104.
27) W. Gąsior, Z. Moser and J. Pstruś: J. Phase. Equil., **22** (2001) 20.
28) W. Gąsior, Z. Moser and J. Pstruś: J. Phase. Equil., **24** (2003) 504.
29) L.S. Darken: Trans. AIME., **175** (1948) 184.
30) W. Sutherland: Phil. Mag., **9** (1905) 781.
31) W.F. Gale and T.C. Totemeier: Smithells Metals Reference Book, 2004, 3-4.
32) M. Shiinoki, N. Hashimoto, H. Fukuda, Y. Ando and S. Suzuki: Metall. Mater. Trans. B, (2018) online: DOI: 10.1007/s11663-018-1416-3